Materials Science & Engineering A 558 (2012) 730–736

Contents lists available at SciVerse ScienceDirect

Materials Science & Engineering A

journal homepage: www.elsevier.com/locate/msea

Role of dynamic strain aging in the tensile property, cyclic deformation and fatigue behavior of Z2CND18.12N stainless steel between 293 K and 723 K

Dunji Yu [a], Weiwei Yu [b], Gang Chen [a], Fengmin Jin [a], Xu Chen [a,*]

[a] School of Chemical Engineering and Technology, Tianjin University, Tianjin 300072, China
[b] Suzhou Nuclear Power Institute, Suzhou 240051, China

ARTICLE INFO

Article history:
Received 7 July 2012
Received in revised form
19 August 2012
Accepted 20 August 2012
Available online 28 August 2012

Keywords:
Tensile property
Cyclic behavior
Low cycle fatigue
Dynamic strain aging

ABSTRACT

Tensile properties and cyclic stress–strain response of Z2CND18.12N austenitic stainless steel were investigated at the strain rate of 1×10^{-3}/s in the temperature range between 293 K and 723 K. Low cycle fatigue tests were also carried out at the strain rate of 6×10^{-3}/s at 293 K and 623 K. SEM and TEM analyses were performed on the fatigue specimens. Tensile strength and ductility were found to reduce drastically with the temperature increasing from 293 K to 423 K but almost remained on the same level in the range between 523 K and 723 K. Serrations occurred during the stress approaching the ultimate tensile strength at 623 K and 723 K. The cyclic stress responses at temperatures ranging from 293 K to 623 K were characterized by a rapid initial hardening to the maximum stress, followed by gradual softening, whereas at 723 K continuous cyclic hardening was present. The maximum cyclic hardening ratio, defined as the maximum peak stress divided by the initial peak stress, increased with increasing temperature in the present temperature range. Phenomenological friction and back stresses were derived from an analysis of hysteresis loop shapes using the Cottrell scheme. The results indicated that the increase of back stress was mainly responsible for the cyclic hardening. Fatigue life decreased with increasing strain amplitude at both 293 K and 623 K. Transgranular fracture failure mode was observed at both temperatures. TEM observations revealed that the dislocation structure changed from the cellular structure at 293 K to the planar slip band at 623 K. Dynamic strain aging has been believed to play a significant role in tensile properties, cyclic deformation and fatigue behavior of the material.

1. Introduction

Z2CND18.12N austenitic stainless steel (316 type steel in French grade) is a prospective material used for piping systems in nuclear power plants. A typical service condition for such piping lines in a pressurized water reactor (PWR) of nuclear power plant is the pressure of about 17.5 MPa at 623 K. Considering the normal or abnormal cyclic characterization of mechanical and thermal loads, it is necessary to investigate the cyclic behavior and fatigue property of this material in a wide temperature range.

Dynamic strain aging (DSA), generally described as the interactions between mobile dislocations and diffusing solute atoms in solid solutions [1], has been extensively reported to play a pivotal role in the mechanical performance of 316 type stainless steels over a wide temperature range [2–14], roughly from 473 to 1073 K. The Portevin-Le Chatelier (PLC) effect [15], i.e. jerky flow or serrated stress–strain curve, is the typical manifestation of DSA in monotonic tensile tests under appropriate conditions [2]. When it comes to cyclic deformation, DSA mainly manifests itself by serrations in stress–strain hysteresis loops and positive temperature dependence of cyclic work hardening [3–5,9]. Kim et al. [4] found cyclic hardening magnitude increased with increasing temperature for type 316L stainless steels between 573 and 873 K. Srinivasan et al. [5] observed marked cyclic hardening for a 316LN stainless steel between 773 and 873 K, and serrations in stress–strain hysteresis loops at 873 K with strain rate $<1\times10^{-3}$. DSA has been also reported to affect low-cycle fatigue life [4,7,8]. Kim et al. [4] found that fatigue life increased with adding nitrogen at high temperature, and assumed that nitrogen retards DSA. Hong et al. [8] concluded that DSA reduced the fatigue resistance by ways of multiple crack initiation in a cold-worked 316L stainless steel. As mentioned previously, a typical operation temperature is 623 K for Z2CND18.12N steel which is right in the regime of DSA for type 316 stainless steels, so it is necessary to investigate whether DSA affects its mechanical behavior. To our knowledge, published literature focused on the DSA in Z2CND18.12N steel is scarce.

In this paper, monotonic tensile and fully reversed cyclic behavior of Z2CND18.12N stainless steel were investigated under various

* Corresponding author. Tel.: +86 22 27408399; fax: +86 22 27403389.
E-mail address: xchen@tju.edu.cn (X. Chen).

0921-5093/$ - see front matter © 2012 Elsevier B.V. All rights reserved.
http://dx.doi.org/10.1016/j.msea.2012.08.088

uniaxial loading conditions in the temperature range from 293 to 723 K at which DSA may take place. Low-cycle fatigue (LCF) tests were also conducted at 293 K and 623 K, respectively, to study the role of DSA in the fatigue behavior. SEM and TEM analyses were performed on fatigue specimens to elucidate the microstructure characterization.

2. Material and experiments

2.1. Material and specimen

The chemical composition (wt%) of Z2CND18.12N austenitic stainless steel used in this study was as follows: C:0.025; Si:0.430; Mn:1.211; P:0.021; S:0.003; Ni:12.073; Cr:17.517; Mo:2.388; B:0.001; Cu:0.075; Co:0.035; N:0.070 and balance Fe. Solid bars with 18 mm in diameter were cut from original pipes for PWR nuclear power plants along the axial direction, and then were machined into dog-bone type specimens with gage section 10 mm in diameter and gage length of 40 mm in accordance with ASTM standard E606-04. The specimen surface was polished along the longitudinal direction, using emery paper down to #2000 (about 13 μm), so as to remove surface defects such as machining marks.

2.2. Test apparatus

Tests were carried out on a closed-loop servo-hydraulic fatigue test machine (MTS810) with a radiant heating furnace that controls the temperature accuracy in a range of $\pm 2\,^{\circ}C$. Strains were measured and controlled by a MTS high temperature extensometer with a gauge length of 25 mm.

2.3. Test procedures

All tests were conducted in air. Tensile tests were under two forms of displacement control (i.e. extensometer control and crosshead control) in sequence. Extensometer control for the strain rate of 1×10^{-3}/s ended at the strain of 30% at room temperature and 8% at 423 K, 523 K, 623 K and 723 K. Thus, effective length was determined by the extensometer control, and then crosshead control continued until failure at the speed of 1.8 mm/min, corresponding to the nominal strain rate of 1×10^{-3}/s. Engineering strain was obtained by dividing the displacement to the effective length. Fully reversed strain cycling tests were conducted for 100 cycles with the strain amplitude of 0.6% and the strain rate of 1×10^{-3}/s at different temperatures between 293 K and 723 K. LCF tests with different strain amplitudes from 0.3% to 0.6% were conducted at the strain rate of 6×10^{-3}/s at room temperature and 623 K, respectively. Fracture surfaces of the fatigue specimens were examined using SEM. TEM were performed on the thin foils cut along the longitudinal direction from the gage length section of the specimens. The thin foils were first mechanically polished down to 50 μm, and then further thinned using a Precision Ion Polishing System.

3. Experimental results

3.1. Tensile behavior

Stress–strain diagrams of the tensile tests are shown in Fig. 1. As seen from Fig. 1(a), the material exhibited a typical three-stage behavior during monotonic tension at all temperatures: a rapid hardening that is almost linear before the strain of about 10%, then a relatively slow nonlinear hardening to a saturated stress, i.e. the ultimate tensile strength, and finally a drastic drop of stress until failure. It is interesting to notice from Fig. 1(b) that serrations occurred at 623 K and 723 K when the stress was approaching the tensile strength. Serrations at 723 K were more intense than those at 623 K.

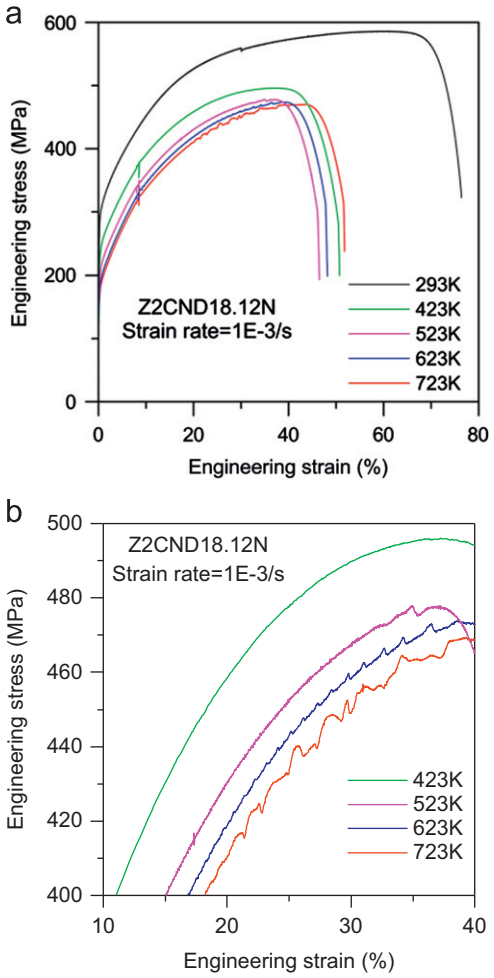

Fig. 1. Stress–strain curves of the tensile tests at the strain rate of 1×10^{-3}/s: (a) full range profiles and (b) sections in large scale before the stress approaches the ultimate strength.

Table 1
Tensile properties of Z2CND18.12N steel at the strain rate of 1×10^{-3}/s.

Temperature (K)	Elastic modulus (GPa)	0.2% Proof stress (MPa)	Ultimate tensile strength (MPa)	Elongation (%)
293	190	291	586	76.38
423	180	232	496	50.71
523	170	203	478	46.46
623	161	183	474	48.19
723	155	174	471	51.78

Mechanical properties obtained from Fig. 1 is given in Table 1. It can be seen that the elastic modulus and 0.2% proof stress decreased with increasing temperature. The elongation decreased from 76.38% at 293 K to 51.06% at 423 K, and almost remained on the same level of about 50% between 423 K and 723 K. Meanwhile, after a sharp drop from 586 MPa at 293 K to 496 MPa at 423 K, the ultimate tensile strength decreased relatively slowly to 478 MPa at 523 K, and then showed little change with temperature increasing to 723 K.